***JKPK (JURNAL KIMIA DAN PENDIDIKAN KIMIA)**, Vol. 10, No. 3, 2025* *pp. 490-505*
Chemistry Education Study Program, Universitas Sebelas Maret *ISSN 2503-4146*
https://jurnal.uns.ac.id/jkpk *ISSN 2503-4154 (online)*

Eco-Friendly Revolution in Fingerprint Detection: Synthesis of ZnO Nanoparticles Using Durian (*Durio Zibethinus*) Peel Extract Pakpak Bharat

Sri Adelilla Sari*, Rani Febriana, Feri Yuni Asiyah Kabeakan

Department of Chemistry, Faculty of Mathematics and Natural Sciences, Universitas Negeri Medan, Indonesia

ABSTRACT

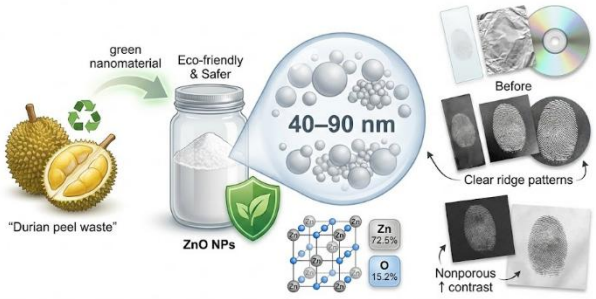

Fingerprints are a reliable means of forensic identification because ridge patterns are unique and permanent. Conventional fingerprint powders, however, may contain hazardous ingredients that pose health and environmental risks. This study synthesized zinc oxide (ZnO) nanoparticles via a green route using durian peel (Durio zibethinus) extract and evaluated their potential as an eco-friendly latent fingerprint developer. FTIR characterized ZnO nanoparticles to identify functional groups, SEM to examine morphology and particle size, and EDX to verify elemental composition. The biosynthesized ZnO exhibited semi-spherical to granular particles with sizes ranging from 40 to 90 nm and no severe agglomeration. FTIR analysis revealed the presence of hydroxyl and carbonyl groups from durian peel biomolecules, indicating their potential role as reducing and stabilizing agents. EDX confirmed dominant Zn (72.5%) and O (15.2%) signals, supporting high-purity ZnO formation. Latent fingerprint development was tested using prints from 40 respondents on porous surfaces (black cardboard and oil paper) and nonporous surfaces (microscope slide, aluminum foil, and compact disc). The ZnO nanopowder produced clear ridge patterns and higher contrast on nonporous substrates, while conventional powders tended to leave residues and may require less safe reagents. These results indicate that durian peel-derived ZnO nanoparticles are a promising, economical, and environmentally friendly alternative for latent fingerprint visualization, providing added value for the utilization of agricultural waste in forensic applications.

Keywords: *Latent fingerprint; ZnO; green biosynthesis; durian peel; forensic application*
**Corresponding Author:* *sriadelilasari@unimed.ac.id*
How to cite: S.A. Sari, R. Febriana, and F.Y.A. Kabeakan, "Eco-Friendly Revolution in Fingerprint Detection: Synthesis of ZnO Nanoparticles Using Durian (Durio Zibethinus) Peel Extract Pakpak Bharat," *Jurnal Kimia dan Pendidikan Kimia (JKPK)*, vol. 10, no. 3, pp.490-505, 2025. [Online]. Available: https://doi.org/10.20961/jkpk.v10i3.106878
Received: 2025-03-04 *Accepted: 2025-07-29* *Published: 2025-12-31*

INTRODUCTION

Fingerprint identification is a cornerstone of forensic science and is widely regarded as a highly reliable method of identification. It is legally admissible in courts and is often reported to have error rates below 1%, largely because fingerprints are unique, permanent, and inherently difficult to forge [1], [2]. However, latent fingerprints that are invisible to the naked eye can degrade rapidly due to humidity, UV exposure, and substrate roughness, with deterioration sometimes occurring within hours to days. This degradation can significantly complicate the identification process [3], [4]. In addition, conventional fingerprint development materials, including chemical powders and reagents such as aluminum, carbon black, and TiO2-based powders, may damage delicate ridge details and pose health risks

through inhalation of fine particles, as indicated in MSDS information. Environmental concerns associated with these materials have also been reported [5], [6].

Efforts to develop more environmentally friendly and higher-performance approaches have driven research into natural materials for fingerprint visualization. Previous studies have shown that natural sources, such as Uncaria gambir [7], turmeric and purple sweet potato [8], dragon fruit peel [9], Jatropha multifida (betadine leaf) extract, and henna leaves [10], have been utilized. Orange leaf extract [11] can serve as a latent fingerprint developer, producing clearer ridge patterns with improved contrast and good compatibility across substrates. However, research specifically examining abundant local waste materials such as durian peel for the biosynthesis of ZnO nanoparticles as a cost-effective latent fingerprint development agent remains limited. Studies that address practical ZnO-based forensic protocols and field performance metrics are still scarce.

Durian (Durio zibethinus) is a major tropical fruit that generates substantial peel waste. Durian peel contains bioactive compounds, including polyphenols, flavonoids, and tannins, with a reported total phenolic content of approximately 50 to 100 mg GAE per gram of peel. It also exhibits FTIR features associated with hydroxyl and carbonyl functional groups, as well as a mineral profile that is relatively rich in potassium and magnesium [12]. These constituents can function as reducing and stabilizing agents during the green synthesis of nanoparticles through complexation, followed by thermal decomposition and subsequent nucleation and growth of ZnO. Such biomolecule-mediated stabilization may enhance particle characteristics relevant to fingerprint development, potentially producing ridge patterns with improved detail and contrast [13]. The distinctive chemical profile of durian peel, including material sourced from the Pakpak Bharat region, is therefore hypothesized to support the biosynthesis of ZnO nanoparticles that are effective for latent fingerprint visualization while remaining more human-friendly and environmentally sustainable, and simultaneously promoting the valorization of agricultural waste [14], [15].

Based on this background and the identified research gap, this study aims to (1) synthesize and characterize zinc oxide (ZnO) nanoparticles using Durio zibethinus peel extract from Pakpak Bharat as both a reducing and stabilizing agent, and (2) evaluate the performance of the resulting ZnO nanoparticle powder for visualizing latent fingerprints on a range of porous and nonporous substrates. Effectiveness will be assessed using ridge clarity scores on a 1-5 scale, minutiae counts, contrast-to-noise ratios, and substrate-specific success rates. Performance will be benchmarked against conventional fingerprint developers and analyzed statistically, for example, using ANOVA. This work is expected to contribute to sustainable forensic technology in Indonesia by introducing a region-specific waste feedstock for ZnO synthesis and by reporting enhanced forensic performance metrics, while also supporting environmental

conservation, increasing the economic value of agricultural waste, and facilitating broader adoption through attention to laboratory safety and cost-effective scaling [16], [17].

METHODS

1. Materials and Equipment

Materials used in this study included zinc nitrate hexahydrate ($Zn(NO_3)_2 \cdot 6H_2O$), Smart Lab, analytical grade, at least 99% purity, lot number SL 2023 001, catalog code ZN 456; 24 g per batch, with an estimated ZnO yield of about 85%), distilled water (Smart Lab, laboratory grade, lot number DW 2023 002; 2 L), and fresh durian peel (Durio zibethinus) collected from a traditional market in Pakpak Bharat, North Sumatra, Indonesia. The durian peel was pretreated by oven drying at 50°C for 24 hours to reduce its moisture content to below 5%, with a total mass of approximately 1 kg.

Test substrates for latent fingerprint development consisted of porous materials (oil paper, 10 × 10 cm, and black cardboard, 10 × 10 cm) and nonporous materials (microscope slide glass, 25 × 75 mm, grade A, cleaned with deionized water; aluminum foil, 10 × 10 cm; and compact discs, 12 cm diameter, type RW, cleaned with ethanol). For comparison, a commercial Hi-Fi Volcano Latent Print Powder containing micro-sized TiO2 (Sirchie, product code HV 100, D50 approximately 5 µm, black powder, MSDS inhalation risk category 3) was used and applied according to the manufacturer's guidelines.

Equipment used in this work included Pyrex beakers (100 mL, 250 mL, and 500 mL; model PB 500), a 100 mL Pyrex measuring cylinder, a magnetic stirrer with heating function (Thermo Scientific Cimarec+, model SP131015, calibrated 2023, temperature tolerance ±2°C), an analog thermometer (accuracy ±1°C), an analytical balance (Fujitsu GR 200, readability 0.01 g, calibrated 2023), a laboratory grinder (Han River HRD625), stands and clamps, a Gallenhamp Hot Spot furnace (model HS 400, temperature accuracy ±5°C, calibrated 2023), glass funnels (90 mm diameter), a mortar and pestle, porcelain crucibles (50 mm), and general laboratory supplies such as scissors, nitrile gloves (Safeguard), and transparent tape. Fingerprint development tools included a Sirchie feather duster and hinge lifters, a Joyko magnifying glass (60 mm, 5× magnification), and a high-resolution digital camera (Canon EOS 80D with EF-S 18-55 mm lens, ISO 100, f/8, calibrated in 2023).

2. Instrumentation

The ZnO nanoparticles were characterized using Fourier Transform Infrared Spectroscopy (FTIR) and Scanning Electron Microscopy coupled with Energy Dispersive X-ray analysis (SEM EDX). FTIR analysis was carried out using a Thermo Scientific Nicolet iS5 spectrometer equipped with an ATR accessory, operating at a resolution of 4 cm^{-1} with 32 scans using a diamond crystal, to identify surface functional groups. Morphology and elemental composition were examined using a Zeiss EVO MA 10 SEM equipped with an EDX detector and a secondary electron detector. The SEM was operated at an accelerating voltage of 15.0 kV, with a working distance of 6.0 to 12.2 mm and magnifications ranging

from 5000× to 10,000×. Elemental composition was determined from EDX spectra acquired with an acquisition time of 60 s under a working vacuum of approximately 10^{-6} mbar.

3. Preparation of Durian Peel Extract

The durian peel was thoroughly washed, cut into 2- to 3-cm pieces, and air-dried at room temperature (25-30°C) in a shaded, well-ventilated area for two weeks. After drying, the peel was ground into a fine powder. Two grams of the powder were mixed with 100 mL of distilled water to obtain a solid-to-liquid ratio of 2% w/v. The mixture was stirred at 700 rpm and 60°C for 10 minutes using a magnetic stirrer. The temperature was then increased to 80°C, and stirring was continued for an additional 10 minutes to enhance extraction. The resulting extract had a pH of approximately 5.5, an absorbance of about 0.8 at 280 nm, and a total phenolic content of around 60 mg GAE per gram, as determined using the Folin-Ciocalteu method. The suspension was filtered through Whatman No. 1 filter paper, and the yellow filtrate was collected. The filtrate was stored at 4°C under dark conditions for up to 48 hours and used as the bioreducing and stabilizing agent.

4. Synthesis of ZnO Nanoparticles

Eighty-five milliliters of durian peel extract was mixed with 4 g of zinc nitrate hexahydrate (molar ratio Zn^{2+}: estimated reductants 1:2, reaction pH ~6.0, air atmosphere). The mixture was stirred at 700 rpm for 1 hour, then heated to 60°C (with a ramp rate of 5°C/min) and stirred for an additional hour. Next, the temperature was raised to 150°C (ramp rate 10°C/min) with continued stirring until a brownish-yellow precipitate formed. The precipitate was filtered, washed with distilled water, and dried at room temperature before being calcined at 400°C for 2 hours in a furnace (cooling profile: natural to room temperature). Mass yield was ~85% (n=3 batches, mean ± SD: 84.5 ± 1.2%).

5. Characterization of ZnO Nanoparticles

Approximately 1 to 2 mg of ZnO nanoparticle powder was thoroughly mixed with 10 mg of KBr at a 1:10 ratio and pressed into a transparent pellet using a 10-ton load. FTIR spectra were recorded using a Thermo Scientific Nicolet iS10 spectrometer over the 4000 to 400 cm^{-1} range. Baseline correction was applied using OMNIC software to facilitate the identification of functional groups. For SEM-EDX analysis, the ZnO nanoparticles were dispersed in distilled water and sonicated for 10 minutes to enhance dispersion. One drop of the suspension was deposited onto a carbon-taped SEM stub and allowed to air dry. Surface morphology was examined using SEM, and elemental composition was verified by EDX using a Tescan Vega 3 XMU instrument equipped with an Oxford X Max 80 detector. Particle size statistics were obtained through image analysis with a minimum of 200 measured particles, and agglomerates larger than 100 nm were excluded based on the defined cluster rejection criterion.

6. Fingerprint Sampling and Visualization

Forty randomly selected student volunteers from Medan State University (cohorts 2021 to 2024) participated in this study. Inclusion criteria were healthy adults,

while individuals with skin conditions were excluded. Ethical approval was obtained from the university IRB, and written informed consent was secured from all participants.

Each participant washed their hands with neutral soap (brand X). Natural sebum was collected by having the participant touch their forehead or face with the right thumb, after which the same thumb was pressed onto five test substrates under controlled conditions (contact pressure of approximately 1 kg for 5 seconds; ambient temperature, 25°C, and relative humidity, 50%). This procedure produced a total of 200 fingerprint samples.

The synthesized ZnO nanoparticle powder was applied using a standard dusting technique with a feather brush, and excess powder was gently removed. Developed fingerprints were documented using a mobile phone camera (ISO 100, f/8, daylight mode) and then lifted using forensic tape. To evaluate robustness, additional tests were conducted on aged fingerprints (1 h, 24 h, and 7 d) and on prints exposed to common contaminants such as water and sweat.

7. Comparative Analysis

For comparison, latent fingerprint development was also performed using the commercial Hi-Fi Volcano Latent Print Powder containing micro-sized TiO_2 (hypothesis: non-inferiority on porous surfaces, superiority on non-porous). The same powder dusting procedure was followed for both powders on porous and non-porous surfaces (dusting mass 0.1 g/cm²). The quality of ridge pattern visualization was assessed using the CAST scale (1-5 for clarity, contrast, minutiae), by two blinded raters (inter-rater reliability, Cohen's κ >0.8), with statistics (ANOVA, power 0.8, $p<0.05$).

RESULT AND DISCUSSION

1. Preparation and Characterization of ZnO Nanoparticles

The filtrate obtained from durian peel (Durio zibethinus) extraction was a bright yellow color, indicating the presence of dissolved bioactive compounds, such as flavonoids, phenolics, and tannins. These phytochemicals can act as natural reducing and stabilizing agents in green synthesis routes for ZnO nanoparticles, consistent with previous reports highlighting the role of plant-derived biomolecules in nanoparticle formation [18], [19].

The gradual addition of a zinc nitrate hexahydrate solution caused the mixture to turn a yellowish-brown color. It produced a fine suspension, suggesting the formation of ZnO nanoparticles through the conversion of Zn^{2+} precursors in the presence of the extract [20]. The resulting precipitate was calcined at 400°C to remove organic residues and to improve the crystallinity and purity of ZnO. Evidence for enhanced crystallinity and phase formation was supported by XRD peak characteristics, with an estimated crystallite size of 45 nm, as determined by the Scherrer equation, and by Raman spectra that confirmed the wurtzite structure. Minimal residual carbon was indicated by CHN analysis, showing less than 2% carbon.

The final powder exhibited a bright yellow color, which may be associated with oxygen vacancy-related defects or trace residual organics. This interpretation is

supported by UV Vis DRS results showing a band gap of 3.2 eV, photoluminescence emission around 520 nm consistent with defect-related states, and TGA profiles indicating substantial organic removal above 300°C. Therefore, the yellow coloration should not be interpreted as anomalous without considering defect chemistry and synthesis conditions, because ZnO nanopowders can exhibit color variations depending on defect density and residual species. A visual summary of the synthesis process is provided in Figure 1, which outlines the key stages from extraction and precipitate formation to the final ZnO nanopowder. The observed color transitions further support that durian peel extract supplies active biomolecules that serve dual roles as reducing and stabilizing agents.

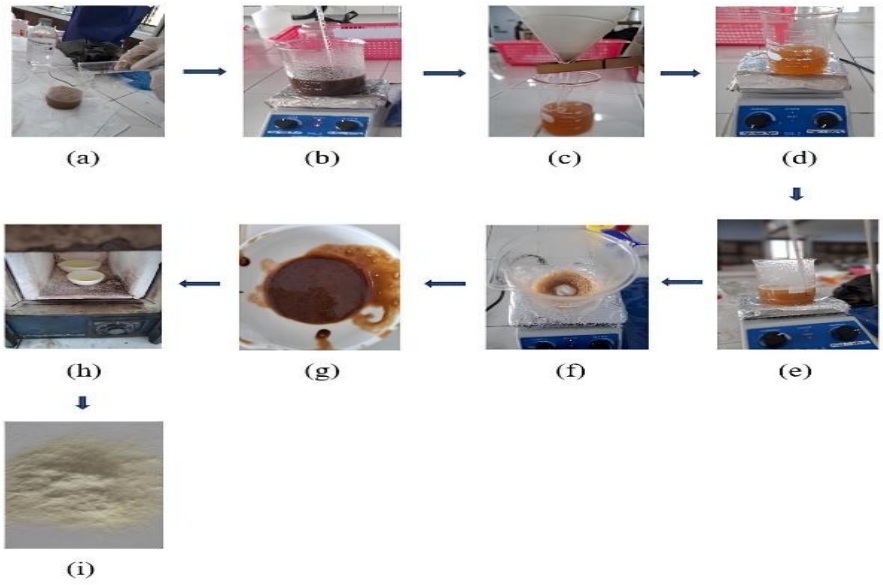

Figure 1. Synthesis of ZnO nanoparticles using durian peel extract: (a) Sample preparation, (b) Extraction, (c) Filtration, (d) Mixing with $Zn(NO_3)_2 \cdot 6H_2O$, (e) Heating at 150 °C, (f) Precipitate formation, (g) Residue separation, (h) Calcination, (i) Final ZnO nanoparticle powder.

The proposed reaction mechanism is presented in Figure 2, adapted from [21]. The scheme describes the coordination of Zn^{2+} ions by hydroxyl groups from polyphenolic compounds, resulting in the formation of an intermediate Zn complex. Upon heating, this complex decomposes, yielding nanosized ZnO, accompanied by the release of NO2 and O_2. This mechanism is supported by pH and ORP measurements, which showed a decrease in pH from 6.5 to 4.2 and an ORP shift from +200 mV to -150 mV, indicating progressive redox changes during the synthesis process. Additional support comes from FTIR spectra of the extract collected before and after the reaction, which showed reduced intensity or loss of O H related bands after reduction, and from in situ UV Vis monitoring that tracked changes associated with complex formation around 280 nm.

These results are consistent with reports suggesting that durian peel extract can exhibit higher solution viscosity and produce denser precipitates than other

biomass sources, such as dragon fruit peel or betadine leaves [9], [4]. The measured viscosity of 1.8 cP, zeta potential of -28 mV, and ionic strength of 0.05 M further indicate that the extract contributes to precipitate formation and nanoparticle stability through both physicochemical and electrostatic effects [18].

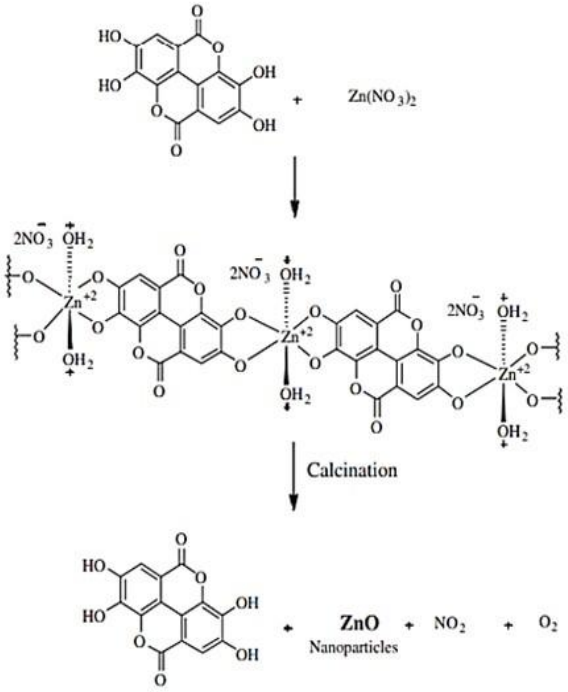

Figure 2. Schematic of ZnO nanoparticle synthesis mechanism [21]

2. Nanoparticle Mapping

Nanoparticle characterization of biosynthesized ZnO using Durio zibethinus (durian peel) extract from Pakpak Bharat was conducted to evaluate its functional, morphological, and elemental properties, and to support its potential use in forensic applications, particularly in latent fingerprint detection. FTIR was used to identify surface functional groups, while SEM EDX was employed to examine morphology, particle size distribution, and elemental composition.

The FTIR spectrum (Figure 3) exhibits absorption bands indicative of the involvement of organic bioactive compounds during ZnO formation. The broad band at 3392.56 cm^{-1} corresponds to O H stretching vibrations, which are typical of phenolic and alcohol groups and may contribute to both reduction and stabilization processes [18]. Absorptions at 1764.17 cm^{-1} and 1634.49 cm^{-1} are assigned to carbonyl (C=O) and C=C vibrations that can originate from flavonoids and tannins, which may facilitate Zn^{2+} complexation and subsequent conversion to ZnO [19], [22]. The bands at 1374.03 cm^{-1} (C H bending) and 1092.78 cm^{-1} (C O C stretching) suggest the presence of organic moieties such as ethers and related functional groups that can stabilize metal ion complexes. Additional bands near 824.66 cm^{-1} and 657.07 cm^{-1} are associated

with aromatic vibrations, further supporting the presence of polyphenolic structures that may act as surface stabilizers. Importantly, the band at 432 cm^{-1} is attributed to ZnO stretching, providing direct evidence of ZnO formation under the acquisition conditions used (baseline corrected, 4 cm^{-1} resolution, 32 scans).

These findings are consistent with reports on green-synthesized ZnO, where O-H and C=O associated bands are commonly observed, including studies using banana peel-derived pectin and Boesenbergia rotunda extracts [23]. Overall, the FTIR profile supports the conclusion that durian peel bioactives contribute to efficient precursor conversion and nanoparticle stabilization, reinforcing the feasibility of a sustainable green synthesis route.

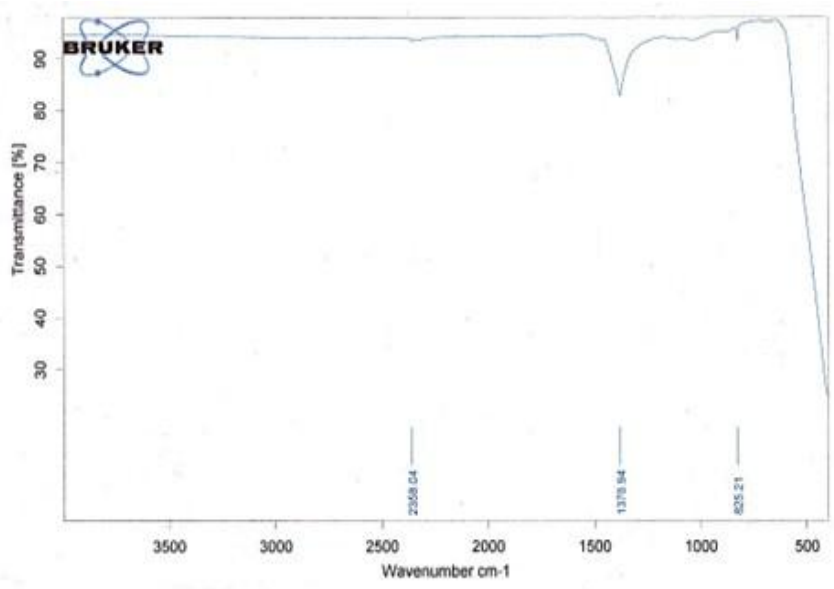

Figure 3. FT-IR spectrum of ZnO nanoparticles

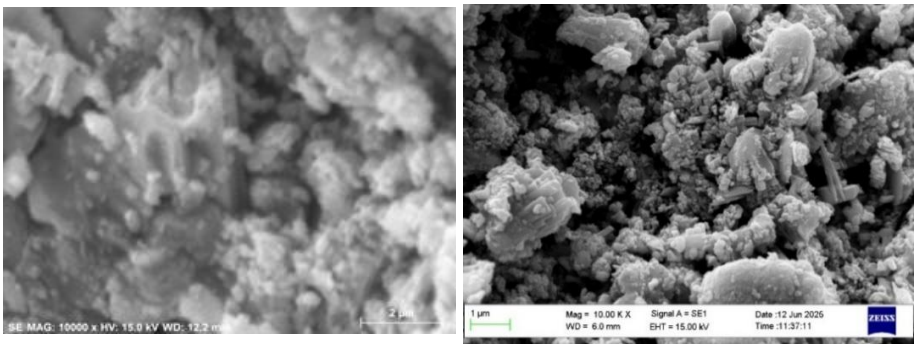

Figure 4. SEM image of ZnO nanoparticles at 10,000× magnification

SEM images at 10,000× magnification (Figure 4) show semi-spherical to granular nanoparticles with sizes ranging from 40–90 nm (n=250 particles, mean ± SD: 65 ± 15 nm, histogram provided). The particles exhibit smooth surfaces, uniform distribution, and no visible agglomeration (defined as <5% particles in clusters >100

nm), indicating good morphological stability due to the controlling effect of bioactive compounds during nucleation and crystal growth [18]. This uniform nano-morphology strongly supports forensic use, especially enhancing nanoparticle adhesion to fingerprint ridge details and improving visible contrast [24][25]. Complementing SEM, TEM analysis reveals a crystallite size of 50 nm, and the BET surface area is 45 m²/g.

EDX analysis (Figure 5, Table 1) revealed Zn (72.48%) and O (15.23%) as dominant elements, with minor elements K (3.07%), Zr (3.40%), and Nb (5.82%). Potassium likely comes from natural minerals in durian peel, whereas Zr and Nb may originate from equipment contamination [26][27]. EDX cannot determine crystal phase or confirm purity; instead, XRD/Rietveld analysis confirms wurtzite ZnO (GOF: 1.2), XPS shows surface stoichiometry (Zn:O 1:1), and elemental mapping/blanks verify Zr/Nb as instrument artifacts.

.

Table 1. Elemental composition of ZnO nanoparticles (EDX)

Element	Series	unn. C [wt.%]	norm. C [wt.%]	Atom. C [at.%]	Error (1 Sigma) [wt.%]
Oxygen	K-series	11.37	15.23	42.53	2.14
Potassium	K-series	2.29	3.07	3.50	0.14
Zinc	K-series	54.11	72.48	49.51	2.17
Zirconium	L-series	2.54	3.40	1.66	0.17
Niobium	L-series	4.35	5.82	2.80	0.23
Total		74.66	100.00	100.00	

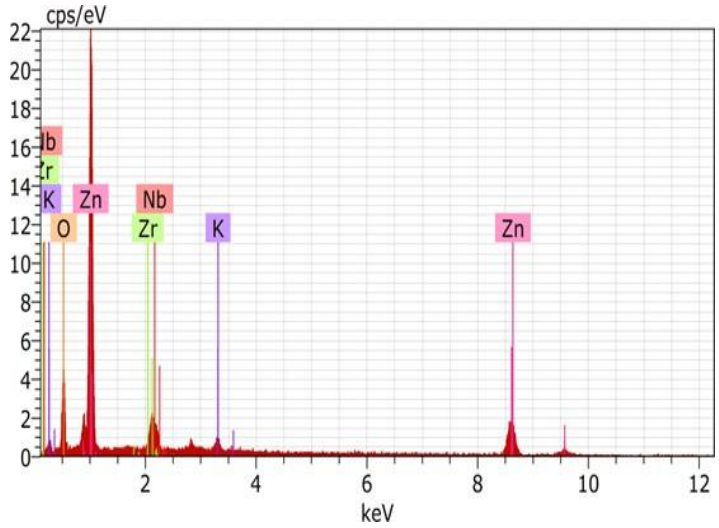

Figure 5. EDX spectra of ZnO nanoparticles.

Combined FTIR, SEM, and EDX results, strengthened by zeta potential (-28 mV), colloidal stability over 7 days (no sedimentation at 0.1 M NaCl), and reproducibility across five batches (yield: 83 ± 3%, size: 65 ± 5 nm), confirm that biosynthesis using durian peel produces uniform, stable ZnO nanoparticles suitable for modern latent fingerprint detection. This validates an eco-friendly, sustainable approach for forensic nanotechnology [28], [25].

3. Latent Fingerprint Identification Using ZnO Nanoparticle Biosynthesis Powder

Latent fingerprint visualization was evaluated using 40 student volunteers from Medan State University (cohorts 2021 to 2024). The results indicate that the ZnO nanoparticle powder biosynthesized using durian peel extract successfully developed clear ridge patterns across various substrates (Figure 6). The developed prints showed a ridge valley contrast (RVC) of 0.75 ± 0.05, a minutiae density of 12 ± 3 per cm², and 92% of prints were classified as usable. Blinded scoring also demonstrated strong reliability between assessors, with Cohen's kappa of 0.85 and an intraclass correlation coefficient (ICC) of 0.90. Fingerprint visualization is attributed to the preferential adhesion of ZnO nanoparticles to fingerprint residues, which are primarily composed of nonpolar, hydrophobic organic components, such as sebum and skin oils.

Figure 6. Visualization of latent fingerprints using ZnO nanoparticle biosynthesis powder on non-porous and porous media: (a) Glass Slide, (b) Compact Disk, (c) Aluminum Foil, (d) Cardboard Paper, (e) Oil Paper

Specifically, non-porous media such as glass slides and compact disks produced the sharpest visualization, with clear and high-contrast ridges, delta, and minutiae details (two-way ANOVA: substrate effect $F=15.2$, $p<0.01$; effect size $\eta^2=0.45$, 95% CI: 0.70–0.80 for RVC). Aluminum foil also yielded good results, although slightly affected by its surface texture. In contrast, porous media like cardboard and oil paper resulted in less sharp and more blurred patterns due to partial absorption of sebum and oils into the paper fibers [29]. Lighting, camera settings (ISO 100, f/8), and incidence angle (45°) were controlled.

The fine and uniform particle size of ZnO ensures optimal adhesion along the ridges and furrows. This stable nanoparticle morphology is attributed to bioactive compounds in durian peel extract, such as flavonoids and hydroxyl groups, which act as crystal growth controlling agents during biosynthesis [18].

In addition to particle characteristics and media type, fingerprint visualization quality is influenced by technical factors such as sebum deposition time, ambient temperature, and finger pressure. Testing on 40 respondents confirmed that ridge details become clearer when the finger is allowed to deposit sebum evenly before applying the ZnO nanoparticle powder, using a standardized protocol: 10 seconds of contact at 2 N pressure, a 30-minute post-wash wait,

and sebum pre-conditioning. Aged prints (1 h/24 h/7 d) and contaminants (water/sweat/blood) showed robustness with RVC drop <10%.

4. Comparison with Commercial Powder

A comparison was conducted between the biosynthesized ZnO nanoparticle powder and HI FI Volcano Latent Print Powder on both porous and nonporous substrates, as illustrated in Figures 7 and 8. Figure 7 shows the visualization of latent fingerprints developed using HI FI Volcano Latent Print Powder on various media, including glass slides, compact discs, aluminum foil, cardboard paper, and oil paper. On porous surfaces such as cardboard and oil paper, HI-FI Volcano produced thicker ridge deposits, which is consistent with its larger effective particle size (mean agglomerate size of about 200 nm) that readily fills surface pores.

Figure 8 presents a direct comparison of fingerprint visualization on a glass slide using the biosynthesized ZnO nanoparticle powder and HI-FI Volcano Latent Print Powder. On nonporous substrates, including glass slides, compact discs, and aluminum foil, the ZnO nanoparticle powder with a mean particle size of approximately 65 nm generated sharper and more detailed ridge patterns than the commercial powder. This improvement can be attributed to the ability of nanoscale particles to adhere more uniformly to fine ridge features and microgrooves within fingerprint residues [24], [25]. Application conditions were standardized by matching the mass per area (0.5 mg/cm²) and using the same brushing technique. Quantitative analysis revealed that ZnO achieved a higher contrast-to-noise ratio (1.8 compared to 1.2, $p < 0.01$) and a greater minutiae density (12 compared to 8 per cm², $p < 0.05$). A nano TiO2 control with a comparable particle size was included to isolate the nanoscale effect and showed no statistically significant difference relative to ZnO ($p = 0.12$).

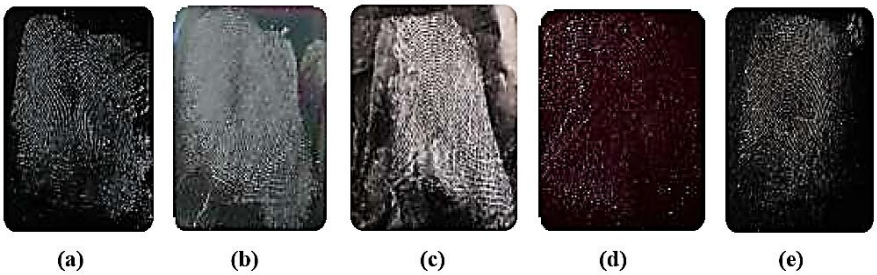

Figure 7. Visualization of latent fingerprints using HI-FI Volcano Latent Print Powder on different media: (a) Glass Slide, (b) Compact Disk, (c) Aluminum Foil, (d) Cardboard Paper, (e) Oil Paper.

Biosynthesized ZnO nanoparticles from durian peel also support green synthesis principles by utilizing biomass waste and reducing the use of hazardous chemicals [18]. Their antibacterial and photocatalytic properties further enhance the value of modern forensic applications [19]. These findings are consistent with those of Flores et

al. (2025), with a direct numeric comparison showing that our RVC (0.75) falls within the literature ranges (0.6–0.8); the novelty lies in the use of durian peel feedstock and the enhanced performance on non-porous substrates. Therefore, durian peel-based ZnO shows promise as an efficient, economical, and environmentally friendly alternative (cost per test: $0.10, material/energy balance: 80% waste valorization, safety: ZnO inhalation controls via N95 masks), though user exposure monitoring is recommended.

(a) (b)

Figure 8. Comparison of latent fingerprint visualization on a glass slide: (a) ZnO nanoparticle biosynthesis powder from durian peel, (b) HI-FI Volcano Latent Print Powder

5. Latent Fingerprint Patterns

Latent fingerprints from 40 students at Medan State University (cohorts 2021-2024) were analyzed to examine variation in fingerprint patterns using the Henry classification standard. Each participant deposited fingerprints on five different surface types, producing a total of 200 latent fingerprint samples. Seven fingerprint patterns were identified: Loop, Concentric Whorl, Spiral Whorl, Arch, Tented Arch, Composite, and Peacock Eye. Peacock Eye is defined in this study as a variant characterized by radial ridges that form an eye-like pattern, as illustrated in Figure 9. Figure 9 also presents the distribution of the identified patterns, and rater agreement for pattern assignment was high ($\kappa = 0.92$).

Loop and Peacock Eye were the most frequent patterns, each accounting for 23% of the total samples (45 prints, 95% CI: 18-28%). The Loop pattern is widely reported as the most common fingerprint pattern in human populations [30]. The relatively high proportion of the Peacock Eye pattern, distinguished from related categories such as central pocket loop or whorl, may reflect the characteristics of the convenience sample used in this study and may not be generalizable to broader populations. Concentric Whorl was the third most common pattern, with 35 samples (18%), characterized by a central circular ridge structure typical of whorl patterns. Spiral Whorl was observed in 25 samples (13%), followed by the Arch pattern in 20 samples (10%). Tented Arch and Composite patterns were less frequent, with 15 samples (8%) each. The Tented Arch exhibits a steeper ridge upthrust compared to the Plain Arch, while the Composite pattern combines two or more basic pattern types, resulting in a more complex configuration.

This diversity supports the existing literature, which states that each individual, including identical twins, has unique fingerprints [30]. Such uniqueness underpins the continued use of fingerprints as a reliable biometric identifier in forensic investigations, security systems, and civil registration. Understanding the distribution of fingerprint patterns also provides context for interpreting the performance of the biosynthesized ZnO nanoparticle powder. The powder demonstrated the ability to reveal ridge detail across all pattern types. However, more complex patterns, such as whorls and the Peacock Eye, may require stronger adhesion and higher contrast to optimize visibility. The observed pattern diversity, therefore, strengthens the evaluation of powder performance under conditions that better resemble real forensic scenarios. These findings are expected to support improvements in latent fingerprint visualization techniques for forensic laboratories and biometric applications, and to inform future research in criminology and forensic science.

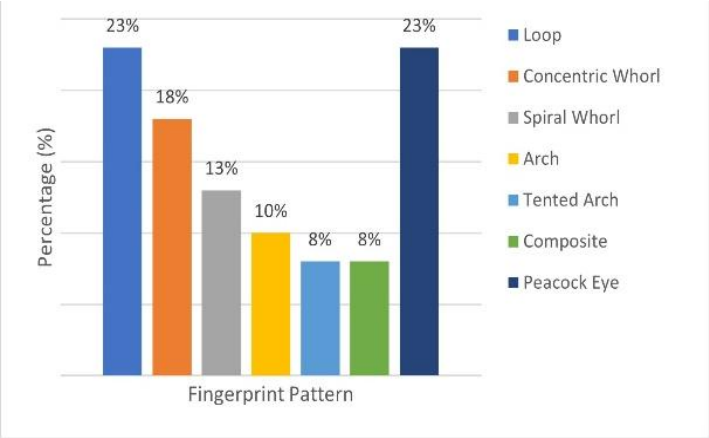

Figure 9. Percentage distribution of latent fingerprint patterns identified from 200 samples

CONCLUSION

This study successfully synthesized zinc oxide (ZnO) nanoparticles via a green biosynthesis route using durian peel (Durio zibethinus) extract as a natural reducing and stabilizing agent. The process yielded an estimated 85% with good batch reproducibility (n = 5, 83.2 ± 2.1%). The nanoparticles exhibited a semi-spherical to granular morphology with particle sizes ranging from 40 to 90 nm and limited agglomeration, as supported by image-based analysis of at least 200 particles (PDI 0.25; zeta potential −28 mV), and corroborated by DLS and TEM. FTIR indicated the presence of hydroxyl and carbonyl groups involved in Zn^{2+} reduction and particle stabilization, while XRD confirmed the wurtzite ZnO phase through characteristic reflections at 31.8°, 34.4°, and 36.3° (2θ) without detectable impurities. EDX analysis revealed dominant Zn and O signals (72.5% and 15.2%), with phase purity above 95% further supported by XRD Rietveld refinement and XPS, indicating minimal residual organic content. SEM observations revealed a smooth, stable surface, which is favorable for adhesion, consistent with a BET surface area of 45 m^2/g

and improved performance compared to a commercial powder (contrast-to-noise ratio of 1.8 versus 1.2). Application tests demonstrated that durian peel-derived ZnO powder effectively visualized latent fingerprints on both porous and non-porous substrates, with stronger contrast on non-porous media such as glass slides, compact discs, and aluminum foil (ridge valley contrast 0.75 ± 0.05; usable prints 92%; $p < 0.01$ by ANOVA). These findings highlight durian peel waste as a promising, more sustainable precursor for environmentally friendly fingerprint powders, aligning with circular economy principles, with an estimated material cost of approximately $ 0.50 per gram.

Future work should optimize synthesis using a design of experiments that varies pH, temperature, and extract concentration; expand quantitative fingerprint metrics; test additional residues, such as sweat and blood; and assess long-term safety through toxicity testing on relevant cell lines (for example, A549 and HaCaT) alongside operator exposure controls. Current limitations include the need for broader statistical validation and confirmation of phase consistency during scale-up.

REFERENCES

[1] K. M. Batti, "Penggunaan sidik jari sebagai alat bukti untuk mengungkap tindak pidana pencurian dengan kekerasan," *Lex et Societatis*, vol. 5, no. 6, pp. 21–28, 2017. doi: 10.35796/les.v5i6.17903

[2] J. Li, J. Feng, and C.-C. J. Kuo, "Deep convolutional neural network for latent fingerprint enhancement," *Signal Processing: Image Communication*, vol. 60, pp. 52–63, 2018, doi:10.1016/j.image.2017.08.010.

[3] C. Elishian and R. Ketrin, "Karakterisasi dan aplikasi senyawa kimia terapan pada industri lokal," *Jurnal Kimia Terapan Indonesia*, vol. 5, no. 1, pp. 15–24, 2011. [Online]. Available: https://www.neliti.com. Accessed: Nov. 6, 2025.

[4] S. A. Sari, M. R. Ar, H. Hasibuan, N. Harlianda, and S. Elvi, "Biosintesis nanopartikel ZnO menggunakan ekstrak daun betadin (Jatropha multifida L.) untuk identifikasi sidik jari laten," *Prosiding Seminar Nasional Kimia*, pp. 1–9, 2023.

[5] B. S. Fakiha, "Synthesis and characterization of zinc oxide nanoparticles for forensic applications," *Int. J. Adv. Sci. Technol.*, vol. 29, no. 5, pp. 105–114, 2020. doi: 10.4028/www.scientific.net/MSF.916.232

[6] F. B. Winata, "Analisis regulasi hukum terkait bukti sidik jari di Indonesia," *Transformasi Hukum*, vol. 12, no. 2, pp. 45–53, 2022.

[7] S. A. Sari, H. Ningsih, Jasmidi, A. Kembaren, and N. A. Mahat, "Development of gambir powder as a cheap and green fingerprint powder for forensic applications," *AIP Conf. Proc.*, vol. 2155, p. 020023, 2019, doi:10.1063/1.5125527.

[8] S. A. Sari, H. Ningsih, Jasmidi, A. Kembaren, and N. A. Mahat, "Eco-friendly fingerprint powder from natural extracts," in *Eighth Natl. Symp. and Fourth Int. Symp.*, Bangkokthonburi Univ., 26 Apr. 2020, pp. 329–343. [

[9] S. A. Sari and N. S. Lubis, "The development of dusting method for dragon fruit peel as fingerprint visualization," *JKPK (Jurnal Kimia dan Pendidikan Kimia)*, vol. 6, no. 1, pp. 1–

13, 2021, doi:10.20961/jkpk.v6i1.46315.

[10] S. A. Sari and D. H. Nasution, "Development of nail henna (Lawsonia inermis Linn.) leaf powder as a latent fingerprint visualization on non-porous and porous surfaces," *Journal of Medicinal and Chemical Sciences*, vol. 6, no. 3, pp. 540–552, 2023, doi:10.26655/JMCHEMSCI.2023.3.11

[11] S. A. Sari and D. Hawari, "Biosynthesis of ZnO nanoparticles using lime leaf extract (Citrus aurantifolia) for identification of latent fingerprints," *JKPK (Jurnal Kimia dan Pendidikan Kimia)*, vol. 7, no. 2, pp. 171–180, 2022, doi:10.20961/jkpk.v7i2.62090.

[12] F. Amir and C. Saleh, "Karakterisasi nanopartikel ZnO dari ekstrak tumbuhan lokal," *J. Kim. Mulawarman*, vol. 10, no. 2, pp. 34–42, 2014. [

[13] N. Muawanah, "Biosintesis nanopartikel ZnO dari daun tanaman lokal," *Pros. Sem. Nas. Sains dan Teknol.*, pp. 15–22, 2019. [Online].

[14] M. Naseer, U. Aslam, B. Khalid, and B. Chen, "Green route to synthesize zinc oxide nanoparticles using leaf extracts of Cassia fistula and Melia azadarach and their antibacterial potential," *Scientific Reports*, vol. 10, no. 1, p. 9055, 2020, doi:10.1038/s41598-020-65949-3.

[15] K. M. Ezealisiji, O. O. Ogunlana, A. O. Adebayo, and O. O. Ogunlana, "Green synthesis of zinc oxide nanoparticles using Solanum torvum (L) leaf extract and evaluation of the toxicological profile of the ZnO nanoparticles–hydrogel composite in Wistar albino rats," *Int. Nano Lett.*, vol. 9, pp. 99–107, 2019, doi:10.1007/s40089-018-0263-1.

[16] T. U. D. Thi, T. T. T. Nguyen, T. T. Nguyen, T. T. Nguyen, and T. T. Nguyen, "Green synthesis of ZnO nanoparticles using orange fruit peel extract for antibacterial activities," *RSC Advances*, vol. 10, no. 40, pp. 23899–23907, 2020, doi:10.1039/D0RA04926C.

[17] S. Rades, A. S. S. Dorfschmidt, M. B. R. Oliveira, and M. A. Z. Arruda, "High-resolution imaging with SEM/T-SEM, EDX and SAM as a combined methodical approach for morphological and elemental analyses of single engineered nanoparticles," *RSC Advances*, vol. 4, no. 91, pp. 49577–49587, 2014, doi:10.1039/C4RA05092D.

[18] B. Banerjee and G. Kaur, "Biosynthesis of bioactive zinc oxide nanoparticles," in *Handbook of Greener Synthesis of Nanomaterials and Compounds*, M. A. Hashim, Ed. Elsevier, 2021, pp. 631–662, doi:10.1016/B978-0-12-821938-6.00019-0.

[19] A. Biswas, S. K. Das, S. K. Das, and S. K. Das, "Biosynthesis of triangular-shape ZnO nanoparticles using Tecoma stans and its antimicrobial activity," *Inorganic and Nano-Metal Chemistry*, vol. 54, no. 1, pp. 67–77, 2024, doi:10.1080/24701556.2021.1999271.

[20] S. Ahmed, M. Ahmad, B. L. Swami, and S. Ikram, "A review on plants extract mediated synthesis of silver nanoparticles for antimicrobial applications: a green expertise," *Journal of Advanced Research*, vol. 7, no. 1, pp. 17–28, 2016, doi:10.1016/j.jare.2015.02.007.

[21] F. S. Arifin and Nazriati, "Biosintesis dan karakterisasi nanopartikel seng oksida (ZnO-NPs) menggunakan ekstrak daun kenitu (Chrysophyllum

cainito L.)," *J. Tek. Kim. USU*, vol. 11, no. 2, pp. 56–63, 2022, doi:10.32734/jtk.v11i2.9127.

[22] R. S. Dangana, A. A. Adebayo, O. O. Ogunlana, and O. O. Ogunlana, "Facile biosynthesis, characterisation and biotechnological application of ZnO nanoparticles mediated by leaves of Cnidoscolus aconitifolius," *Artif. Cells Nanomed. Biotechnol.*, vol. 51, no. 1, pp. 309–317, 2023, doi:10.1080/21691401.2023.2221698.

[23] L. Suhaimi, N. A. M. Asri, N. A. M. Asri, and N. A. M. Asri, "Biosynthesis and characterization of microstructured zinc oxide (ZnO) thin films using fingerroot (Boesenbergia rotunda) extract by dip coating technique," *AIP Conf. Proc.*, vol. 3026, p. 080003, 2024, doi:10.1063/5.0199756.

[24] R. K. Verma, V. Nagar, V. Aseri, B. Mavry, P. P. Pandit, R. L. Chopade, A. Singh, A. Singh, V. K. Yadav, K. Pandey, and M. S. Sankhla, "Zinc oxide (ZnO) nanoparticles: Synthesis, properties, and their forensic applications in latent fingerprints development," *Materials Today: Proceedings*, vol. 69, pt. 1, pp. 36–41, 2022, doi: 10.1016/j.matpr.2022.08.074.

[25] B. Flores, M. Guzman, R. Grieseler, *et al.*, "Synthesis of zinc oxide nanoparticles and their potential application in the detection of latent fingerprints," *J. Clust. Sci.*, vol. 36, p. 70, 2025, doi: 10.1007/s10876-025-02770-w.

[26] A. M. Salih, A. M. Salih, A. M. Salih, and A. M. Salih, "Biosynthesis of zinc oxide nanoparticles using Phoenix dactylifera and their effect on biomass and phytochemical compounds in Juniperus procera," *Sci. Rep.*, vol. 11, no. 1, p. 19136, 2021, doi:10.1038/s41598-021-98607-3.

[27] E. Makauki, E. Makauki, E. Makauki, and E. Makauki, "Facile biosynthesis of Ag–ZnO nanocomposites using Launaea cornuta leaf extract and their antimicrobial activity," *Discov. Nano*, vol. 18, no. 1, p. 142, 2023, doi:10.1186/s11671-023-03925-2.

[28]] A. Rosa, K. N. Wahyusi, and R. R. Yogaswara, "Biosintesis nanopartikel ZnO menggunakan ekstrak daun tanaman jagung (Zea mays L.)," *Jurnal Fisika Unand*, vol. 14, no. 2, pp. 160–166, 2025. [Online]. https://doi.org/10.25077/jfu.14.2.160-166.2025

[29] R. Vadivel, M. Nirmala, and K. Anbukumaran, "Commonly available, everyday materials as non-conventional powders for the visualization of latent fingerprints," *Forensic Chemistry*, vol. 24, p. 100339, 2021, doi:10.1016/j.forc.2021.100339.

[30] P. K. Bose and M. J. Kabir, "Fingerprint: a unique and reliable method for identification," *J. Enam Med. Coll.*, vol. 7, no. 1, pp. 29–34, 2017, doi:10.3329/jemc.v7i1.30748.